ABCC6 Deficiency Promotes Development of Randall Plaque

Emmanuel Letavernier, Gilles Kauffenstein, Léa Huguet, Nastassia Navasiolava, Elise Bouderlique, Ellie Tang, Léa Delaitre, Dominique Bazin, Marta de Frutos, Clément Gay, et al.

ABCC6 deficiency promotes development of Randall's plaque

Emmanuel Letavernier,[1,2,3] Gilles Kauffenstein,[4] Léa Huguet,[1,2] Nastassia Navasiolava,[5] Elise Bouderlique,[1,2] Ellie Tang,[1,2] Léa Delaitre, [5] Dominique Bazin,[6] Marta de Frutos,[6] Clément Gay,[6] Joëlle Perez [1,2] Marie-Christine Verpont, [1,2] Jean-Philippe Haymann,[1,2,3] Viola Pomozi,[7] Janna Zoll,[7] Olivier Le Saux,[7] Michel Daudon,[1,2,3] Georges Leftheriotis, [8] Ludovic Martin [4,5]

[1] Unité Mixte de Recherche S 1155, Sorbonne Universités, Université Pierre et Marie Curie-Paris 06, Paris, France

[2] Unité Mixte de Recherche S 1155, Institut National de la Santé et de la Recherche Médicale, Paris, France

[3] Department of Physiology, Assistance Publique-Hôpitaux de Paris, Hôpital Tenon, Paris, France

[4] Institut des maladies mitochondriales, du coeur et des vaisseaux-MITOVASC, Centre National de la Recherche Scientifique 6015, Institut National de la Santé et de la Recherche Médicale U1083, Angers University,Angers, France

[5] Department of Dermatology, PseudoXanthoma Elasticum Consultation center, Reference Center for rare skin diseases, Angers University Hospital, France

[6] Unité Mixte de Recherche 8502, Laboratoire de Physique des Solides, Centre National de la Recherche Scientifique, Université Paris Sud XI, Orsay, France.

[7] Department of Cell and Molecular Biology, John A. Burns School of Medicine, University of Hawaii, Honolulu, Hawaii

[8] Department of Physiology and Molecular Medicine, Unité Mixte de Recherche 7370Centre National de la Recherche Scientifique, University of Nice, Nice, France

AUTHOR INFORMATION

Correspondence:

Emmanuel LETAVERNIER, Service des Explorations Fonctionnelles Multidisciplinaires, Hôpital TENON, 4 rue de la Chine, 75020 Paris (France). Phone 33 1 56 01 67 73 ; Fax 33 1 56 01 70 03. E-mail: emmanuel.letavernier@aphp.fr

Running Title: ABCC6 and kidney stones

Word Count: 2766 ; Abstract: 239

Number of Figures and Tables: Figures 7 ; Table: 1

Keywords: ABCC6, Kidney stone, Randall's plaque

Disclosure Statement: The authors have nothing to disclose

Significance statement

Pseudoxanthoma Elasticum is a genetic disease caused by *ABCC6* gene mutations resulting in low systemic pyrophosphate levels and soft tissue calcifications. This manuscript describes the presence of massive papillary calcifications (Randall's plaque) and high prevalence of kidney stones in PXE patients. *Abcc6* knock-out mice develop Randall's plaque, demonstrating the major role of pyrophosphate in the prevention of kidney calcifications.

Abstract

Background. Pseudoxanthoma Elasticum (PXE) is a genetic disease caused by *ABCC6* gene mutations resulting in low pyrophosphate levels and subsequent progressive soft tissue calcifications. PXE affects mainly skin, retina and arteries. As many PXE patients experienced kidney stones, we aimed to determine the prevalence of this pathology in PXE patients and to define the possible underlying mechanisms by using murine models.

Methods. A retrospective study was conducted in a large cohort of PXE patients. In addition, urine samples and kidneys from *Abcc6*$^{-/-}$ mice have been analyzed at various ages. Kidney calcifications have been characterized by Yasue staining, Scanning Electron Microscopy, Electron Microscopy coupled to Electron Energy Loss Spectroscopy and µ-Fourier Transform Infrared Spectroscopy.

Results. Among 113 PXE patients, 45 had a past medical history of kidney stones (40%). Computed tomography-scans evidenced massive papillary calcifications (Randall's plaques). *Abcc6*$^{-/-}$ mice spontaneously developed kidney interstitial apatite calcifications with aging, appearing specifically at the tip of the papilla and forming Randall's plaques similar to those observed in human kidneys. *Abcc6*$^{-/-}$ mice had a lower urine excretion of pyrophosphate than controls.

Conclusions. The frequency of kidney stones, and probably Randall's plaque, is extremely high in patients affected by PXE and *Abcc6*$^{-/-}$ mice develop spontaneously interstitial papillary calcifications progressing with age and reminiscent of the human phenotype. *Abcc6*$^{-/-}$ mice thus provide a new and useful model to study Randall's plaque formation. Our findings also highlight a critical role of pyrophosphate in the prevention of Randall's plaque and kidney stones.

Introduction

Pseudoxanthoma elasticum (PXE; OMIM 264800, prevalence 1/25000 to 1/50000) is an autosomal recessive disease resulting from mutations in *ABCC6* gene that encodes an ATP-binding cassette transporter mainly expressed in the liver and to a lesser extent in kidney.[1,2] This disease is characterized by progressive calcification with destruction of the elastic fibers in the skin, retinal Bruch's membrane and the medial layers of large and medium-sized peripheral arteries.

Recent studies have suggested that the hepatic ABCC6 transporter facilitates the release of extracellular ATP, which is quickly converted to inorganic pyrophosphate (PPi) by ectonucleotide pyrophosphatase phosphodiesterase-1 (ENPP1) in the hepatic vasculature. This process is the main source of circulating PPi, a physiological anti-calcifying molecule that counteracts the effect of inorganic phosphate (Pi) on hydroxyapatite (Ca/Pi) crystal growth.[3] Patients with PXE, as well as *Abcc6*$^{-/-}$ mice, have a reduced plasma PPi level, explaining, at least in part, their mineralization disorder.[4-6]

Renal involvement in PXE has been poorly documented in the literature and only sporadic cases of kidney stones in PXE patients have been reported.[7,8] The presence of typical nephrocalcinosis has been reported in one PXE patient.[9] Recently, data from a PXE cohort suggested that nephrolithiasis was an unrecognized but a prevalent feature of PXE, affecting at least 10% of PXE patients.[10] Nevertheless, the prevalence and features of nephrolithiasis have never been specifically assessed.

In order to better characterize the renal calcifications affecting PXE patients we conducted a retrospective study in one of the largest cohorts of PXE patients. We focused on the prevalence of kidney tissue calcifications and kidney stones. In addition, urine samples and kidney tissues from *Abcc6*$^{-/-}$ mice were analyzed to better understand the pathophysiological

mechanisms underlying the development of kidney calcifications in a mouse modelling the human pathology.

Methods

Study population

A national survey was conducted in 164 PXE patients from the PXE Consultation Center of the University Hospital of Angers, France, from December 2016 to June 2017.

The diagnosis of PXE was based on a combination of established criteria for indisputable PXE, including clinically suggestive skin lesions, angioid streaks and histologically proven fragmented and calcified elastic fibers on skin biopsy.[11] Moreover, *ABCC6* genotyping was systematically performed and the all exons of *ABCC6* gene have been sequenced to confirm the diagnosis.[12] Sequence changes were identified in about 85% of alleles. This mutation rate is superimposable to the rate reported in most large cohorts.

The PXE patients were contacted by mail to complete a self-questionaire. All patients with a typical PXE were eligible for inclusion. All patients gave informed written consent and the study was approved by local ethics committee (CPP Ouest II – Angers - France) and registered at ClinicalTrials.gov (Identifier #: NCT01446393).

Six PXE patients who previously experienced renal colic performed a CT-scan to evaluate the presence of remnant stones and Randall's plaque, in various radiology units, and five of them also had urine and blood sample analysis to assess kidney stone risk factors, as recommended by the French Urological Asociation (AFU). Patients sent CT-scans and biological data to Angers reference center managers.

Data collection

The presence of kidney stones and/or nephrocalcinosis, past medical history of kidney stones, renal colic and surgical procedures were recorded. Familial past medical history and stone analysis were also collected when available. Age, height and weight were also collected. eGFR was calculated with the CKD-EPI equation by using the last available plasma creatinine (PCr).[13]

Animal Studies

Mice with a genetically invalidated *Abcc6* gene are designated as Abcc6^{tm1Aabb}. they were generated on a 129/Ola background, backcrossed into a C57Bl/6J background more than 10 times by from Professor Bergen's laboratory.[14] These mice maintained at Angers University mouse facility (France) and at the John A. Burns, school of medicine, University of Hawai'i (USA) are herein designated *Abcc6*$^{-/-}$.

The development of renal calcifications was assessed in 15 *Abcc6*$^{+/+}$ and 17 *Abcc6*$^{-/-}$ female mice housed and bred in similar conditions (5 mice/cage) at the Angers University mouse facility. All animal procedures were performed in accordance with the European Union and NIH Guidelines for the Care and Use of laboratory animals and in accordance with the local ethics committee (CEEA.2012.21). Urine pyrophosphate, calcium, and phosphate excretion were assessed in 9 *Abcc6*$^{+/+}$ and 8 *Abcc6*$^{-/-}$ female mice (12 months-old). Urine was collected by using metabolic cages with free access to water during 24hrs.

In addition, a cDNA encoding the normal human ABCC6 and a PXE-causing mutant ABCC6 cDNA (R1314W) were cloned into delivery plasmids used for transgenic animal production and transgenic mice expressing the normal human ABCC6 protein and the PXE-causing R1314W mutant in the liver were generated at the University of Hawai'i as previously decribed.[15]

Study of the human papillae

Papillae from healthy parts of human kidneys removed for cancer have been analyzed as described in a previous study.[16] This study showed that many patients are affected by incipient Randall's plaque, even in the absence of kidney stones. Patients gave a written consent. Papillae have been anonymously collected and no data relative to patients has been recorded, in accordance to French legislation and Helsinki declaration for Patient Safety.

Morphoconstitutional analysis of renal stones

Morphologic examination and classification of renal stone surface and section were combined with Fourier transform infrared spectroscopy (FTIR, Bruker®).

Histology and Yasue staining of renal tissue

Human and mice kidney tissues were fixed in 4% formalin and embedded in paraffin. Four-µm tissue sections have been performed and stained by Yasue procedure to reveal tissue calcifications. Eosin staining was also performed in addition to Yasue staining to identify red blood cells and vasa recta. Mice papilla calcification ratio has been assessed by isolating the papilla (1.3 mm from the tip) and performing morphometry by Analysis® Software (proportion of calcified tissue/whole papilla).

Field Emission-Scanning Electron Microscopy (FE-SEM)

Tissue sections (4µm) were investigated with a Zeiss SUPRA^{TM}55VP field emission-scanning electron microscope (FE-SEM). Measurements were performed at a low voltage (1.4 keV).

Transmission electron microscopy (TEM).

Small pieces of papilla tip were fixed in 2.5% glutaraldehyde in 0.1 mmol/L cacodylate buffer (pH 7.4) at 4°C. Fragments were then post-fixed in 1% osmium tetroxide, dehydrated using graded alcohol series, and embedded in epoxy resin. Semi-thin sections (0.5 µm) were stained using toluidine blue. Ultrastructure sections (80 nm) were contrast-enhanced using uranyl acetate and lead citrate, and examined using a JEOL 1010 electron microscope (JEOL, Ltd., Tokyo, Japan) with a MegaView III camera (Olympus Soft Imaging Systems GmbH, Münster, Germany).

Electron Energy Loss Spectroscopy (EELS) experiments

EELS experiments were performed in a VGHB01 Scanning Transmission Electron Microscope (STEM) equipped with a cold field emission gun operated at 100 keV. EELS data were collected on a low noise / low temperature CCD camera (Princeton Instruments) optically coupled to a scintillator in the image plane of a Gatan 666 magnetic sector. The sample was cooled down to liquid-nitrogen temperature using a home-made cryo stage.

FTIR micro-spectroscopy

Microcalcifications were characterised using Fourier Transform InfraRed microspectroscopy (µ-FTIR). Tissue sections (4-µm) were deposited on low-emission microscope slides (MirrIR, Keveley Technologies, Tienta Sciences, Indianapolis). FTIR hyperspectral images were recorded with a Spectrum spotlight 400 FT-IR imaging system (Perkin Elmer Life Sciences, Courtaboeuf, France), with a spatial resolution of 6.25 micrometer and a spectral resolution of 8 cm^{-1}. Each spectral image covering a substantial part of the tissue, consisted of about 30,000 spectra.

Mice urine assays

Pyrophosphate assay:

Freshly collected urine samples were centrifuged (10 min 20,000 g 4°C) and supernatant was diluted (1/10 in distilled water) and frozen until use. To quantify PPi, we used ATP sulfurylase to convert PPi into ATP in the presence of excess of adenosine 5' phosphosulfate (APS, Sigma #A5508). Generated ATP was subsequently quantified using ATP Determination Kit (Molecular Probes #A22066) according to the manufacturer instructions.

Urinary creatinine and phosphate have been assessed on an ISYS analyzer from ImmunoDiagnostic Systems. Calcium urinary levels have been measured with the Perkin-Elmer 3300 atomic absorption spectrometer.

Statistical Analyses

Clinical data are presented as mean (SD), median [p25-p75] and percentages and were compared with student t-test and Chi-2 test. Experimental data are presented as mean (SEM) and were compared with non parametric (Mann-Whitney) test. A p value <0.05 was considered significant for all statistics.

Results

High prevalence of kidney stones in PXE patients.

Among the 170 patients participating in the Angers PXE cohort, 164 received the questionnaire and 113 answered the survey (Males:33, Females:80). Among these 113 patients, 45 (39.8 %) had a past medical history of renal colic and/or kidney stones. Forty one patients had kidney stones and 4 patients had renal colic without evidence of kidney stone by imaging. Twenty-eight patients (24.7%) reported at least one case of kidney stone disease in their close family. Kidney stone and non-kidney stones formers characteristics, including estimated renal function (e-GFR; CKD-EPI formula) are summarized in Table 1. There was no significant difference between the 2 groups.

Study of the renal calcifications and urine biochemistry in PXE patients

Six PXE patients from the Angers' cohort who previously experienced renal colic had a Computed Tomography (CT)-scan to assess disease evolution. Urine biochemistry was analyzed in 5 of these 6 kidney stone formers. None of these patients had remnant kidney stone but 5 patients had papillary calcifications (Randall's plaque), as evidenced by CT-scan (Figure 1A-D). One patient had both papillary calcifications and medullary calcifications (incipient nephrocalcinosis, Figure 1E). Urine biochemistry showed mild hypercalciuria in some patients (median 237[122;277] mg/day, normal value<250 mg/day), normal urine phosphate excretion (median 1020[626;1067] mg/day, normal urine oxalate excretion (median 0.36[0.20;0.41] mmol/day) and intermediate urine pH (median 6.2[6.0;6.9]).

Stone analyses

According to the survey, 4 stones have been analyzed in various laboratories and all were made of calcium oxalate, though no detail on stone morphology was obtained. Two other stones from PXE patients passed spontaneously were collected at the Tenon hospital laboratory and a morphoconstitutional analysis of the stone was performed, revealing the presence of massive Randall's plaque remnant within stone umbilication (Figure 1F).

Study of the renal papilla calcifications in *Abcc6*$^{-/-}$ mice

In view of the dramatically high proportion of kidney stone formers among PXE patients, and the presence of Randall's plaque at the origin of these stones, we analyzed whether *Abcc6*$^{-/-}$ mice also developed similar kidney calcifications. Analyses were performed in kidneys from 17 *Abcc6*$^{-/-}$ and 15 wild type mice at various ages: 3±0.5 months; 6±1 months; 12±2 months and 24±2 months (Figure 2 A-F). Yasue staining did not reveal the presence of significant calcifications at any time in wild type animals (Figure 2 E). However, renal calcifications appeared and worsened with aging in *Abcc6*$^{-/-}$ mice papillae (Figure 2A-D, F). At 6 months these calcifications were sparse and located at the most distal part of the papilla, in the interstitium. At 12 months interstitial round-shaped calcifications were developed around tubular structures at the tip of the renal papilla and at 24 months calcifications were important and some tubules were obstructed (n=4 *Abcc6*$^{-/-}$ mice kidneys and n=5 wild type mice kidneys at 24 months, Figure 2 A-D).

Abcc6$^{-/-}$ mice papilla calcifications are similar to human Randall's plaque

Aging *Abcc6*$^{-/-}$ mice developed renal calcifications that were located at the tip of the renal papilla (Figure 3 A, B), resembling human Randall's plaque. Calcification that developed in the kidney interstitial tissue of the *Abcc6*$^{-/-}$ mice were often round-shaped, surrounding loops of Henle and *vasa recta*, similar to calcification observed in human Randall's plaques (Figure

3 C, D). These calcifications were made of spherulites as revealed by scanning electron microscopy, predominating in the interstitial tissue and surrounding vascular and tubular lumens (Figure 3E). Eosin/Yasue staining confirmed that round shaped calcifications developed around both *vasa recta* (containing red blood cells) and around tubular structures with thin epithelium (loops of Henle, Figure 3E). µFourier Transform InfraRed (µFTIR) spectroscopy with an imaging system was used to characterize the chemical phases. The analysis of the absorption spectrum revealed some features specific to the presence of different absorption bands of the apatite [$Ca_5(PO_4)_3(OH)$], especially the ν_3 P-O stretching vibration mode measured at 1035-1045 cm^{-1} (Figure 4 A, B). Carbonate ions were detected together with apatite by their ν_3 C-O stretching vibration mode around 1420 cm^{-1} and the ν_2 C-O bending mode at 875 cm^{-1}. The presence of amorphous calcium phosphate (ACP), revealed by the partial disappearance of the shoulder of the ν_3 P-O absorption band of apatite, was also evidenced (Figure 4 C,D). Finally, calcification was analyzed at the nanometer scale by using transmission electron microscopy coupled to electron energy loss spectroscopy. Interestingly, deposits were located beneath the loops of Henle and *vasa recta* basement membranes. Their structure was frequently concentric and laminated, with mineral layers containing calcium and phosphate but also organic layers. These features were similar to human Randall's plaque (Figure 5 A-C).

Pyrophosphate urinary excretion in *Abcc6*$^{-/-}$ mice

Urine volume and calcium excretion in *Abcc6*$^{-/-}$ mice did not differ from wild-type mice (Figure 6 A-B). Conversely, urine phosphate excretion was slightly but significantly lower in *Abcc6*$^{-/-}$ mice (p=0.027, Figure 6C). Urine pyrophosphate excretion was dramatically reduced in *Abcc6*$^{-/-}$ mice (p=0.009, Figure 6D).

Restoration of systemic pyrophosphate synthesis in *Abcc6*$^{-/-}$ mice protects against Randall's plaque formation

Analyses were performed in kidneys from several 18-months-old transgenic *Abcc6*$^{-/-}$ animals, 3 *Abcc6*$^{-/-}$ mice expressing a PXE-causing ABCC6 mutant protein (R1314W) in the liver and 5 *Abcc6*$^{-/-}$ mice expressing the normal, functional, human ABCC6 protein in the liver. Yasue staining revealed interstitial round-shaped calcifications developed around tubular structures at the tip of the renal papilla in *Abcc6*$^{-/-}$ mice expressing the inactive R1314W mutant. By contrast, mice expressing the normal ABCC6 protein in the liver showed no calcification (Figure 7 A-C, p=0.02).

Discussion

To our knowledge, this is the first study investigating renal stone formation in PXE and suggesting an inhibiting role of pyrophosphate in Randall's plaque formation.

There is evidence that renal stone incidence increased during the past decades in industrialized countries, with a current lifetime prevalence in western countries nearing 10%.[17,18]. Kidney stone prevalence is dramatically increased in PXE patients, affecting ~40% of them. Of note, kidney stone prevalence in the patients close family was much lower. The proportion of kidney stone formers in PXE patients is even more remarkable considering that in the reported literature of PXE, approximately 2 thirds of the patients are women. Indeed, nephrolithiasis generally affects men more frequently than women.[19] Renal function was normal in almost all PXE patients, independently of the presence of kidney stones (Table 1). Remarkably, a recent study identified kidney stones as a feature of PXE but the prevalence was probably underestimated because of the study design. [10]

Randall's plaque is a common mechanism initiating kidney stone formation but the genetic and environmental determinants of Randall's plaque formation are still unknown.[20-22] The observation of massive Randall's plaque by CT-scan in 5/6 PXE patients is a remarkable feature. Only the presence of massive papillary calcifications can be determined by imaging. CT-scans have been performed only in patients with past medical history of kidney stones, but PXE patients without kidney stones may probably also be affected by asymptomatic papillary calcifications. The presence of massive Randall's plaque fragments in the kidney stones from PXE patients suggests that stone formation in these individuals was actually initiated by these plaques. Randall's plaques were first described by Alexander Randall in 1937, who proposed an original theory relative to "The origin and growth of renal calculi".[20] He was the first to identify interstitial calcium phosphate (CaP) deposits at the tip of renal papillae whose growth

resulted in urothelium rupture. Calcium oxalate stones expelled by patients affected by plaques have in some cases a depression due to papilla imprinting and CaP residues, an evidence that stones originate from Randall's plaque.[22,23]

Since the discovery of the implication of *ABCC6* mutations in PXE, a key element in the etiology of this disease has been the recent implication of hepatic, and to a lesser extent renal, ABCC6-mediated ATP release as a major source of circulating pyrophosphate (PPi), a potent calcification inhibitor.[3,24] In the absence of functional ABCC6, PXE patients have low circulating PPi levels leading to ectopic calcifications in the elastic fiber-rich tissues.

Since PPi deficiency increases CaP supersaturation, ABCC6 deficiency could increase CaP supersaturation at the tip of renal papillae and thereby promote Randall's plaque formation in PXE patients.

Urine PPi is not measured in clinical practice, and we were not able to determine PPi urine concentration in PXE stone formers in the absence of a specific protocol. Several studies have described lower PPi concentration in the urine of kidney stone formers.[25-27] Decrease of other calcification inhibitors have also been reported in the urine of kidney stone formers. However, this is the first time to our knowledge that a monogenic defect affecting a calcification inhibitor is associated to an increased risk of Randall's plaque and kidney stone formation in humans.

To test the hypothesis that ABCC6 deficiency and low PPi concentrations would result in Randall's plaque formation, we used the *Abcc6*$^{-/-}$ mouse model that recapitulates many of the pathophysiological and phenotypical characteristics of the human PXE disease. Interestingly, renal calcifications have been previsouly described in the cortex of young *Abcc6*$^{-/-}$ animals, though the medulla and the tip of the renal papilla were not assessed.[28] Kidney calcifications can be "accelerated " by a specific diet (high phosphorus, vitamin D and low magnesium diet) in *Abcc6*$^{-/-}$ young mice, however these calcifications were predominantly located in renal

tubules.[29] It is very likely that the systemic PPi deficiency in these mice in combination with the acceleration diet resulted in massive tubular precipitation of calcium phosphate. These tubular calcifications clearly differ from Randall's plaques observed with aging in *Abcc6*$^{-/-}$ mice, which were mainly found in interstitial tissues and began at the tip of the renal papilla. Remarkably, the renal calcification phenotype we described in aging *Abcc6*$^{-/-}$ mice meets the four essential criteria of Randall's plaque: (i) interstitial deposits around tubular and vessels lumen, (ii) appearing and spreading at the tip of the renal papilla (*i.e.* different from medullary nephrocalcinosis) (iii) made of carbonated apatite and amorphous calcium phosphate, as previously described in human papillae, and (iv) forming nanometer-scale spherulites with both mineral and organic layers.[16]

Interestingly, the development of Randall's plaque in human papillae has been attributed to CaP supersaturation in the interstitial tissue at the tip of the papilla. Asplin *et al.* have hypothesized that CaP supersaturation in the thin limb of Henle's loop could promote CaP particle precipitation.[30] The main determinants of CaP supersaturation *in vivo* are actually high pH, high calcium and phosphate concentrations, and possibly low concentration of calcification inhibitor concentrations.[31] To date, only high urine calcium concentration (hypercalciuria) has been related to the development of plaques at the surface of renal papillae.[32] Since calcium and phosphate concentrations are predicted to be extremely high at the tip of the papilla, inhibitors of crystallization are probably physiologically essential to prevent calcifications in this specific area of the kidney. Our previous attempt to develop Randall's plaques in murine models by inducing hypercalciuria through high vitamin D and calcium intakes have failed. As observed in other hypercalciuric rat models, animals developed CaP stones but no Randall's plaque, despite high CaP supersaturation in urine.[33,34] Of note, PXE patients affected by Randall's plaque had only mild increase in calcium and normal oxalate and phosphate urine concentration, suggesting that hypercalciuria was

probably not the main determinant of CaP supersaturation and plaque formation in these patients. Based on our results, it appears that calcification inhibitors are probably essential to prevent tissue mineralization in kidney. It is remarkable that the invalidation of a single gene (*ABCC6*) promotes Randall's plaque formation, suggesting that PPi is a significant inhibitor of Randall's plaque and kidney stone formation *in vivo*.

PXE is a rare disease but Randall's plaque and related stones are extremely frequent in the general population. Further studies will be necessary to assess whether patients affected by Randall's plaques have low PPi concentration in urine. In our experience, these studies will require special experimental procedures because of low PPi concentration in urine and to pre-analytical pitfalls in our experience (unpublished data). Of note, PPi level in *Abcc6*$^{-/-}$ mice urine was dramatically reduced but we also observed a small but significant decrease in urine phosphate excretion. Further study of phosphate and pyrophosphate homeostasis in PXE patients and *Abcc6*$^{-/-}$ mice is warranted. ABCC6 is expressed in renal proximal tubular cells at a relatively low level.[35] It may be hypothesized that renal ABCC6 could play a role in renal calcifications. However, transgenic *Abcc6*$^{-/-}$ mice expressing a functional human ABCC6 protein were protected against kidney calcifications at 18 months of age, suggesting that raising plasma PPi in these mice, even modestly, exerts a systemic protection.[15] Interestingly, urolithiasis is independently associated to vascular calcifications and increased cardiovascular risk.[36] Whether plasma PPi deficiency could increase both kidney stone and vascular calcifications in kidney stone formers deserves further studies.

Our work presented some limitations. There was a potential bias from an overrepresentation of kidney stone-related episodes in the patient surveys. However, 46 patients reported kidney stones: even if considering the (unlikely) hypothesis that none of the 51 patients who did not reply to the questionnaire were affected by stones, at least 28% (46/164) of PXE patients were affected by stones. This proportion is still extremely high compared to the general population.

Furthermore, even as we observed plaque imprints on kidney stones, we have no evidence that all stones originated from a Randall's plaque. Finally, this type of survey is not adequate to collect extensive clinical data (history of stones, number of episodes, familial medical history...).

In conclusion, we report a dramatic prevalence of kidney stones in patients affected by PXE, a disease notably characterized by low circulating PPi levels. When available, kidney stones and CT-scans revealed the presence of massive Randall's plaques, the first step of kidney stone formation. PXE patients should be aware that they are at high risk to form kidney stones and preventive measures should now be considered (increased diuresis, lowering calcium urinary excretion…). Moreover, *Abcc6*$^{-/-}$ mice, that are also characterized by low circulating and urine PPi levels, develop spontaneously Randall's plaque with age, at the tip of the renal papilla. These observations from a rare monogenic disease suggest that PPi is a major protective factor against the development of Randall's plaque and urolithiasis, a condition affecting 10% of the population. It has been recently demonstrated that PPi administration increases blood PPi levels and protects against tissue calcifications in *Abcc6*$^{-/-}$ mice.[15] Further studies would be useful to assess whether PPi administration may also protect against the development of Randall's plaque in murine models and could therefore be a potential new treatment against kidney stones.

Acknowledgements

We thank Prof. Claude Marsault for his kind relecture of patient CT-scans. We thank PXE patients and PXE France support group, and Mrs Hélène Humeau for her help (data collection). Financial support to Dominique Bazin came from ANR grant ANR-12-BS08-0022. Financial support to Olivier Le Saux came from NIH grants HL108249 and P20GM113134. Financial support to Emmanuel Letavernier came from ANR grant ANR-13-JSV1-0010-01, and from Société de Néphrologie (Genzyme grant), Académie Nationale de Médecine (Nestlé-Waters award), Convergence-UPMC CVG1205 and CORDDIM-2013-COD130042.

Authors contribution

EL, GK, OLS, MD, GL and LM designed the study
EL, GK, LH, NN, EB, ET, LD, DB, MDF,CG, JP, MCP, JPH, VP, JZ, OLS, MD, LM carried out experiments and clinical research
EL, GK, LH, NN, ET, JP, MDF, CG, JP, OLS,MD, GL, LM analyzed the data
EL, GK, LH, MDF, CG, DB, OLS made the figures
EL, GK, OLS, GL, MD and LM drafted and revised the paper
All authors approved the final version of the manuscript

Financial Conflict of Interest: none

References

1: Li Q, Jiang Q, Pfendner E, Váradi A, Uitto J: Pseudoxanthoma elasticum: clinical phenotypes, molecular genetics and putative pathomechanisms. *Exp Dermatol* 18: 1-11, 2009

2: Le Saux O, Urban Z, Tschuch C, Csiszar K, Bacchelli B, Quaglino D, Pasquali-Ronchetti I, Pope FM, Richards A, Terry S, Bercovitch L, de Paepe A, Boyd CD: Mutations in a gene encoding an ABC transporter cause pseudoxanthoma elasticum. *Nat Genet* 25: 223-227, 2000

3: Jansen RS, Duijst S, Mahakena S, Sommer D, Szeri F, Váradi A, Plomp A, Bergen AA, Oude Elferink RP, Borst P, van de Wetering K: ABCC6-mediated ATP secretion by the liver is the main source of the mineralization inhibitor inorganic pyrophosphate in the systemic circulation-brief report. *Arterioscler Thromb Vasc Biol* 34: 1985-1989, 2014

4: Vanakker OM, Leroy BP, Coucke P, Bercovitch LG, Uitto J, Viljoen D, Terry SF, Van Acker P, Matthys D, Loeys B, De Paepe A: Novel clinico-molecular insights in pseudoxanthoma elasticum provide an efficient molecular screening method and a comprehensive diagnostic flowchart. *Hum Mutat* 29: 205, 2008

5: Ziegler SG, Ferreira CR, MacFarlane EG, Riddle RC, Tomlinson RE, Chew EY, Martin L, Ma CT, Sergienko E, Pinkerton AB, Millán JL, Gahl WA, Dietz HC: Ectopic calcification in pseudoxanthoma elasticum responds to inhibition of tissue-nonspecific alkaline phosphatase. *Sci Transl Med* 9: 393, 2017

6: Zhao J, Kingman J, Sundberg JP, Uitto J, Li Q: Plasma PPi Deficiency Is the Major, but Not the Exclusive, Cause of Ectopic Mineralization in an Abcc6(-/-) Mouse Model of PXE. *J Invest Dermatol* 17: 31665-31672, 2017

7: Fabre B, Bayle P, Bazex J, Durand D, Lamant L, Chassaing N: Pseudoxanthoma elasticum and nephrolithiasis. *J Eur Acad Dermatol Venereol* 19: 212-215, 2005

8: Mallette LE, Mechanick JI: Heritable syndrome of pseudoxanthoma elasticum with abnormal phosphorus and vitamin D metabolism. *Am J Med* 83:1157-1162, 1987

9: Seeger H, Mohebbi N: Pseudoxanthoma elasticum and nephrocalcinosis. *Kidney Int* 89: 1407, 2016

10: Legrand A, Cornez L, Samkari W, Mazzella JM, Venisse A, Boccio V, Auribault K, Keren B, Benistan K, Germain DP, Frank M, Jeunemaitre X, Albuisson J: Mutation spectrum in the ABCC6 gene and genotype-phenotype correlations in a French cohort with pseudoxanthoma elasticum. *Genet Med* 19: 909-917, 2017

11: Lebwohl M, Neldner K, Pope FM, De Paepe A, Christiano AM, Boyd CD, Uitto J, McKusick VA: Classification of pseudoxanthoma elasticum: report of a consensus conference. *J Am Acad Dermatol* 30: 103-107, 1994

12: Leftheriotis G, Kauffenstein G, Hamel JF, Abraham P, Le Saux O, Willoteaux S, Henrion D, Martin L: The contribution of arterial calcification to peripheral arterial disease in pseudoxanthoma elasticum. *PLoS One* 9: e96003, 2014

13: Levey AS, Stevens LA, Schmid CH, Zhang YL, Castro AF 3rd, Feldman HI, Kusek JW, Eggers P, Van Lente F, Greene T, Coresh J; CKD-EPI (Chronic Kidney Disease Epidemiology Collaboration): A new equation to estimate glomerular filtration rate. *Ann Intern Med* 150: 604-612, 2009

14: Gorgels TG, Hu X, Scheffer GL, van der Wal AC, Toonstra J, de Jong PT, van Kuppevelt TH, Levelt CN, de Wolf A, Loves WJ, Scheper RJ, Peek R, Bergen AA: Disruption of Abcc6 in the

mouse: novel insight in the pathogenesis of pseudoxanthoma elasticum. *Hum Mol Genet* 14: 1763-1773, 2005

15: Pomozi V, Brampton C, van de Wetering K, Zoll J, Calio B, Pham K, Owens JB, Marh J, Moisyadi S, Váradi A, Martin L, Bauer C, Erdmann J, Aherrahrou Z, Le Saux O: Pyrophosphate Supplementation Prevents Chronic and Acute Calcification in ABCC6-Deficient Mice. *Am J Pathol* 187: 1258-1272, 2017

16: Verrier C, Bazin D, Huguet L, Stéphan O, Gloter A, Verpont MC, Frochot V, Haymann JP, Brocheriou I, Traxer O, Daudon M, Letavernier E: Topography, Composition and Structure of Incipient Randall Plaque at the Nanoscale Level. *J Urol* 196: 1566-1574, 2016

17: Sorokin I, Mamoulakis C, Miyazawa K, Rodgers A, Talati J, Lotan Y: Epidemiology of stone disease across the world. *World J Urol* 35: 1301-1320, 2017

18: Stamatelou KK, Francis ME, Jones CA, Nyberg LM, Curhan GC: Time trends in reported prevalence of kidney stones in the United States: 1976-1994. *Kidney Int* 63: 1817-1823, 2003

19: Daudon M: [Epidemiology of nephrolithiasis in France]. *Ann Urol (Paris)* 39: 209-231, 2005

20: Randall A: The origin and growth of renal calculi. *Ann Surg* 105: 1009-1027, 1937

21: Evan AP, Lingeman JE, Coe FL, Parks JH, Bledsoe SB, Shao Y, Sommer AJ, Paterson RF, Kuo RL, Grynpas M: Randall's plaque of patients with nephrolithiasis begins in basement membranes of thin loops of Henle. *J Clin Invest* 111: 607-616, 2003

22: Daudon M, Bazin D, Letavernier E: Randall's plaque as the origin of calcium oxalate kidney stones. *Urolithiasis* 43: 5-11, 2015

23: Letavernier E, Vandermeersch S, Traxer O, Tligui M, Baud L, Ronco P, Haymann JP, Daudon M: Demographics and characterization of 10,282 Randall plaque-related kidney stones: a new epidemic? *Medicine (Baltimore)* 94: e566, 2015

24: Jansen RS, Küçükosmanoglu A, de Haas M, Sapthu S, Otero JA, Hegman IE, Bergen AA, Gorgels TG, Borst P, van de Wetering K: ABCC6 prevents ectopic mineralization seen in pseudoxanthoma elasticum by inducing cellular nucleotide release. *Proc Natl Acad Sci USA* 110: 20206-20211, 2013

25: Fleisch H: Inhibitors and promoters of stone formation. *Kidney Int* 13:361-371, 1978

26: Roberts NB, Dutton J, Helliwell T, Rothwell PJ, Kavanagh JP: Pyrophosphate in synovial fluid and urine and its relationship to urinary risk factors for stone disease. *Ann Clin Biochem* 29: 529-534, 1992

27: Muñoz JA, López-Mesas M, Valiente M: Minimum handling method for the analysis of phosphorous inhibitors of urolithiasis (pyrophosphate and phytic acid) in urine by SPE-ICP techniques. *Anal Chim Acta* 658: 204-208, 2010

28: Klement JF, Matsuzaki Y, Jiang QJ, Terlizzi J, Choi HY, Fujimoto N, Li K, Pulkkinen L, Birk DE, Sundberg JP, Uitto J. Targeted ablation of the abcc6 gene results in ectopic mineralization of connective tissues. *Mol Cell Biol* 25: 8299-8310, 2005

29: Li Q, Chou DW, Price TP, Sundberg JP, Uitto J: Genetic modulation of nephrocalcinosis in mouse models of ectopic mineralization: the Abcc6(tm1Jfk) and Enpp1(asj) mutant mice. *Lab Invest* 94: 623-32, 2014

30: Asplin JR, Mandel NS, Coe FL: Evidence of calcium phosphate supersaturation in the loop of Henle. *Am J Physiol* 270: F604-13, 1996

31: Bird VY, Khan SR: How do stones form? Is unification of theories on stone formation possible? *Arch Esp Urol* 70: 12-27, 2017

32: Kuo RL, Lingeman JE, Evan AP, Paterson RF, Parks JH, Bledsoe SB, Munch LC, Coe FL: Urine calcium and volume predict coverage of renal papilla by Randall's plaque. *Kidney Int* 64: 2150-2154, 2003

33: Letavernier E, Verrier C, Goussard F, Perez J, Huguet L, Haymann JP, Baud L, Bazin D, Daudon M: Calcium and vitamin D have a synergistic role in a rat model of kidney stone disease. *Kidney Int* 90: 809-817, 2016

34: Bushinsky DA, Parker WR, Asplin JR: Calcium phosphate supersaturation regulates stone formation in genetic hypercalciuric stone-forming rats. *Kidney Int* 57: 550-560, 2000

35: Beck K, Hayashi K, Nishiguchi B, Le Saux O, Hayashi M, Boyd CD: The distribution of Abcc6 in normal mouse tissues suggests multiple functions for this ABC transporter. *J Histochem Cytochem* 51: 887-902, 2003

36: Shavit L, Girfoglio D, Vijay V, Goldsmith D, Ferraro PM, Moochhala SH, Unwin R: Vascular calcification and bone mineral density in recurrent kidney stone formers. *Clin J Am Soc Nephrol* 10: 278-285, 2015

Figure and Table Legends

Figure 1: PXE patients are affected by massive Randall's plaque.

CT-scans showed papilla calcifications in PXE patients who have been previously affected by kidney stones (Arrows, Figure 1A-D, representative CT-scans from 3 individuals). Among 6 PXE patients who underwent CT-scans, 5 had several papillary calcifications in both right and left kidney (Figure 1C, number of calcified papilla in each individual). One PXE patient was affected by moderate and atypical nephrocalcinosis (cortical calcifications: arrows, Figure 1E). Monohydrate calcium oxalate stone (brown crystalline phase) from a PXE patient with evidence of papilla umbilication and Randall's plaque fragments (white crystalline phase, arrow) (Figure 1F).

Figure 2: Yasue staining evidencing the development of murine Randall's plaque with age. Representative papilla from *Abcc6*$^{-/-}$ mice at various ages exhibit increasing Yasue staining with aging, which was absent in control mice (Magnification x100, Figure 2A-E). The percentage of papillary tissue calcification was assessed by morphometry in 15 wild type (WT) and 17 *Abcc6*$^{-/-}$ mice (Figure 2F). At 24 months, calcified surface was significantly increased in *Abcc6*$^{-/-}$ mice (p=0.01, n = 4 *Abcc6*-/- mice kidneys and n=5 WT mice kidneys).

Figure 3: Calcification is electively located at the tip of the papilla, mainly in the interstitial tissue around capillaries (*vasa recta*) and loops of Henle. Calcification in *Abcc6*$^{-/-}$ mice wasspecifically located at the tip of the papilla (Arrows, Figure 3A, B). Yasue staining performed on papilla slices revealed round-shaped and circular structures surrounding tubules (Magnification x200 and zoom, Figure 3C, D). The structures are similar observed in human papillae from patients affected by Randall's plaque (Magnification x200, Figure 3E). Scanning electron microscopy revealed spherulites in the interstitial tissue, around vasa recta containing red blood cells (*) and loops of Henle (Figure 3F). Eosin plus Yasue staining confirmed that calcifications affect both vasa recta containing red blood cells (white arrow, Figure 3G) and loops of Henle (black arrow, Figure 3G).

Figure 4: Calcifications is made of apatite and amorphous calcium phosphate. µFTIR analysis and imaging of plaques. µFTIR spectra revealed the presence of apatite (Figures 4A, B) but also the presence of mixed apatite with amorphous calcium phosphate-ACP (Figure 4C, D). Figures 4B and 4D are Yasue-stained sections corresponding to area analysed by FTIR.

Figure 5: Nanostructure of calcifications is similar to human Randall's plaque**.** TEM and EELS analysis of murine Randall's plaques. TEM revealed the presence of many small dense deposits often close to endothelial cells and vasa recta (Figures 5A, B). Some concentric and laminated microcalcifications classically described in Randall's plaque have also been observed (Figure 5C). EELS analysis revealed the presence of CaP laminations in these particles, alternating with nitrogen (N)-rich organic layers (Figure 5). (Ca=calcium cartography, P=Phosphorus cartography, N= Nitrogen cartography).

Figure 6: *Abcc6*$^{-/-}$ mice have a low urine pyrophosphate excretion. pH, phosphate, calcium (indexed to urine creatinine) and Pyrophosphate (PPi) urine excretion has been assessed in *Abcc6*$^{-/-}$ and WT mice (N= 8 and 9 animals, respectively, Figure 6A-D). PPi excretion was significantly lower in *Abcc6*$^{-/-}$ mice (Figure 6D, p= 0.009). Urine phosphate excretion was also significantly decreased but to a lower extent (Figure 6C, p=0.027).

Figure 7: Transgenic (tg) ABCC6 expression protects *Abcc6*$^{-/-}$ mice against kidney calcification. Expression of the functional human ABCC6 protein in *Abcc6*$^{-/-}$ mice protected against papillary calcification (Figure 7A, Yasue staining, magnification x100). Expression of the PXE-causing ABCC6 mutant protein (R1314W) did not prevent the development of calcifications in the papilla, which was similar to that observed in *Abcc6*$^{-/-}$ mice (Figure 7B, Yasue staining, magnification x400). The percentage of papillary tissue calcification has been assessed by morphometry in 5 *Abcc6*$^{-/-}$ tg ABCC6 and 3 *Abcc6*$^{-/-}$ tg R1314W mice (Figure 7C). At 18 months of age, calcified surface was significantly decreased in *Abcc6*$^{-/-}$ tg ABCC6 mice (p=0.02).

Table 1: Characteristics and estimated glomerular filtration rate (CKD-EPI formula) in PXE patients affected or not by kidney stones. Data are means±SD; CKD-EPI: estimated glomerular filtration rate.

Table 1: General characteristics of PXE patients

	All PXE patients who fulfilled questionnaire (n=113)	**Patients with medical history of kidney stone (n=45)**	**Patients without medical history of kidney stone (n=68)**
Age (Yrs)	50.1±16.5	50.3±12.5	49.9±18.8
Gender (m/f)	33/80 (29% m)	13/32 (29% m)	20/48 (29% m)
Weight (kg)	67.6±17.5	69.9±21.0	66.1±14.8
Height (cm)	163.6±9.1	164.8±8.8	162.9±9.4
Plasma creatinine (µmol/L)	66.1±12.2	68.4±12.1	64.5±12.2
CKD-EPIcr, ml/min/1.73m²	98.6±17.8	96±14.4	100.2±19.7

Data are means±SD; CKD-EPIcr, estimated glomerular filtration rate

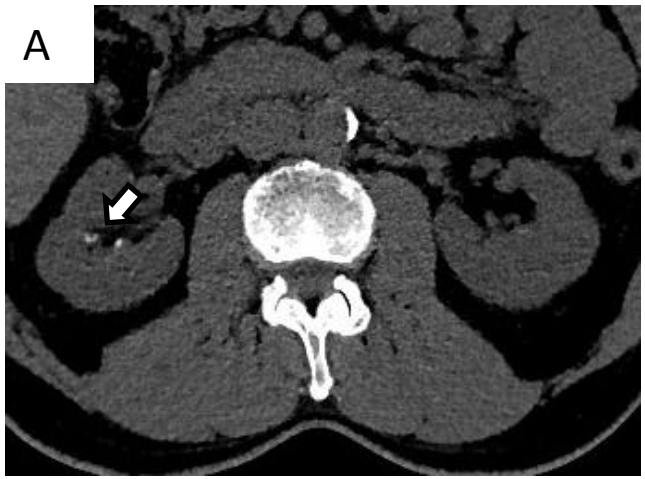
A

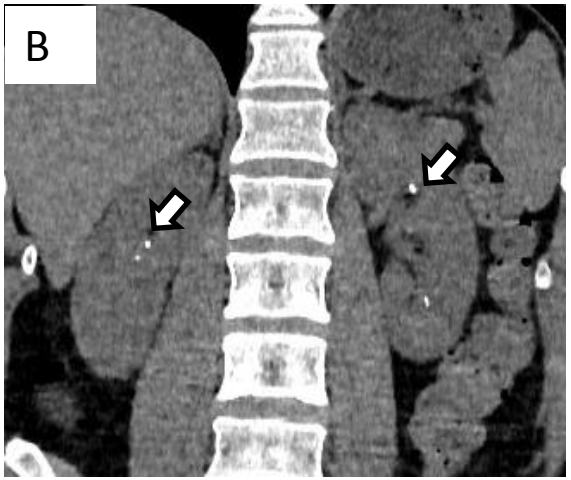
B

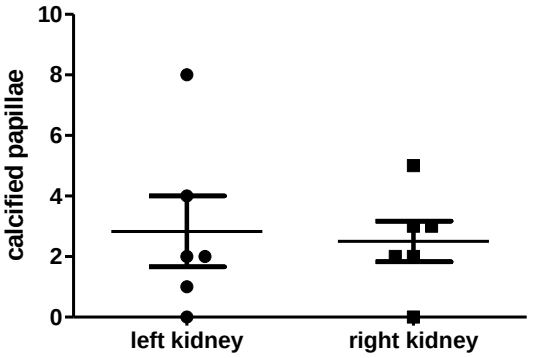
C
calcified papillae
10
8
6
4
2
0
left kidney
right kidney

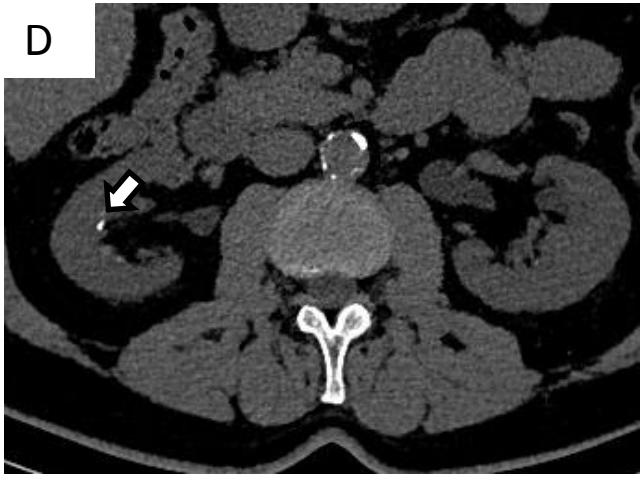
D

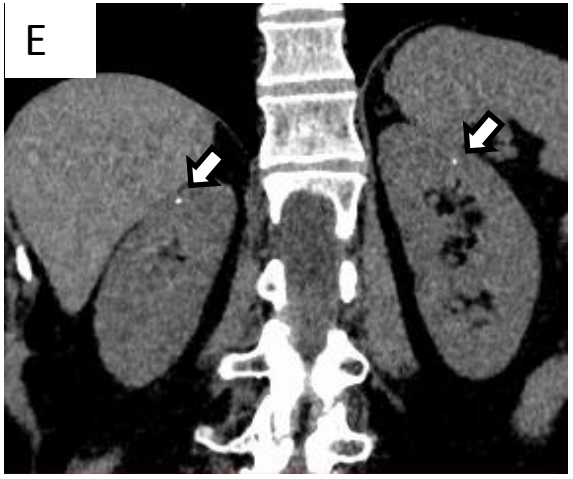
E

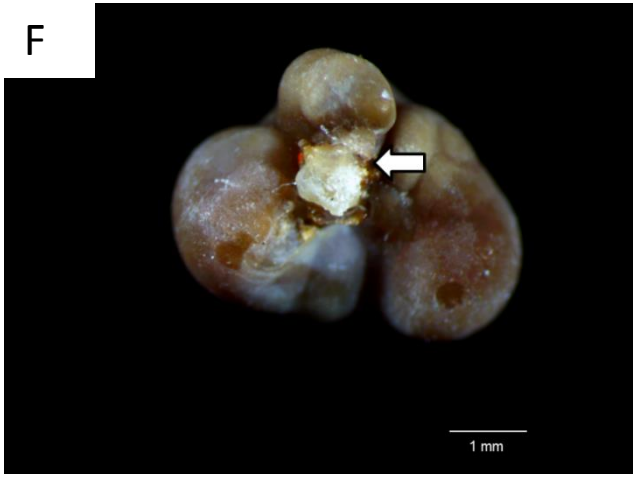
F
1 mm

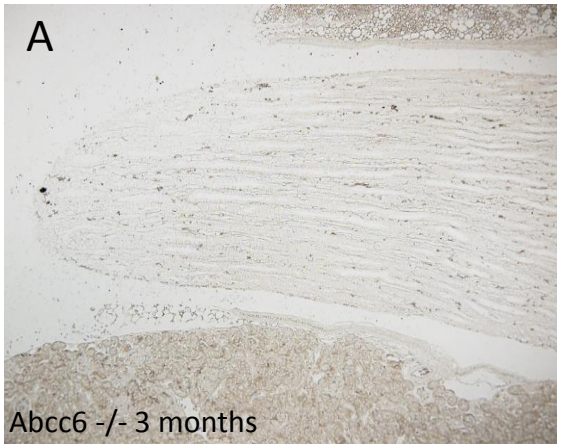
A
Abcc6 -/- 3 months

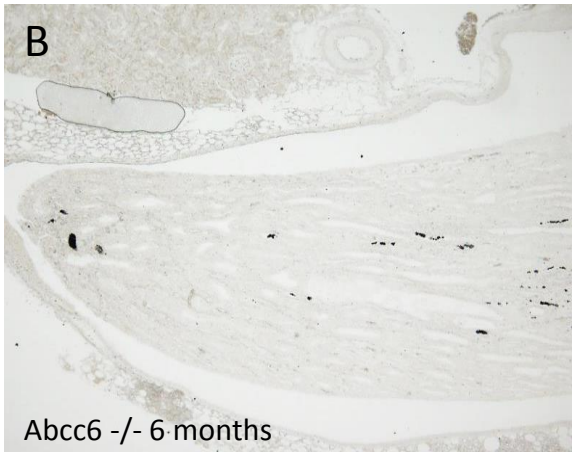
B
Abcc6 -/- 6 months

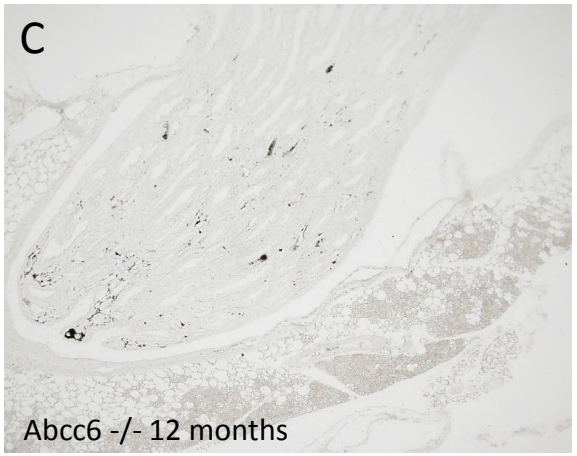
C
Abcc6 -/- 12 months

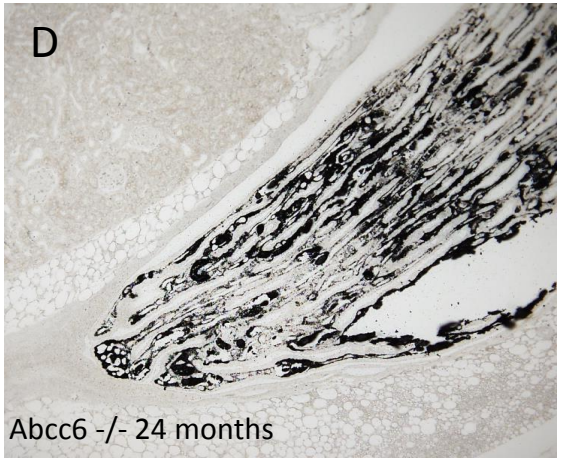
D
Abcc6 -/- 24 months


E
Control 24 months

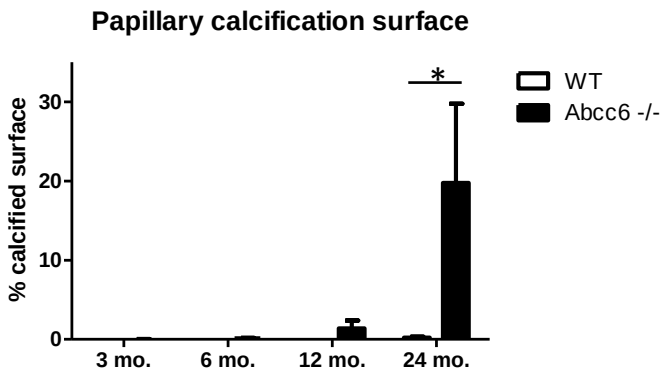
F
Papillary calcification surface
% calcified surface
30
20
10
0
3 mo.
6 mo.
12 mo.
24 mo.
*
WT
Abcc6 -/-

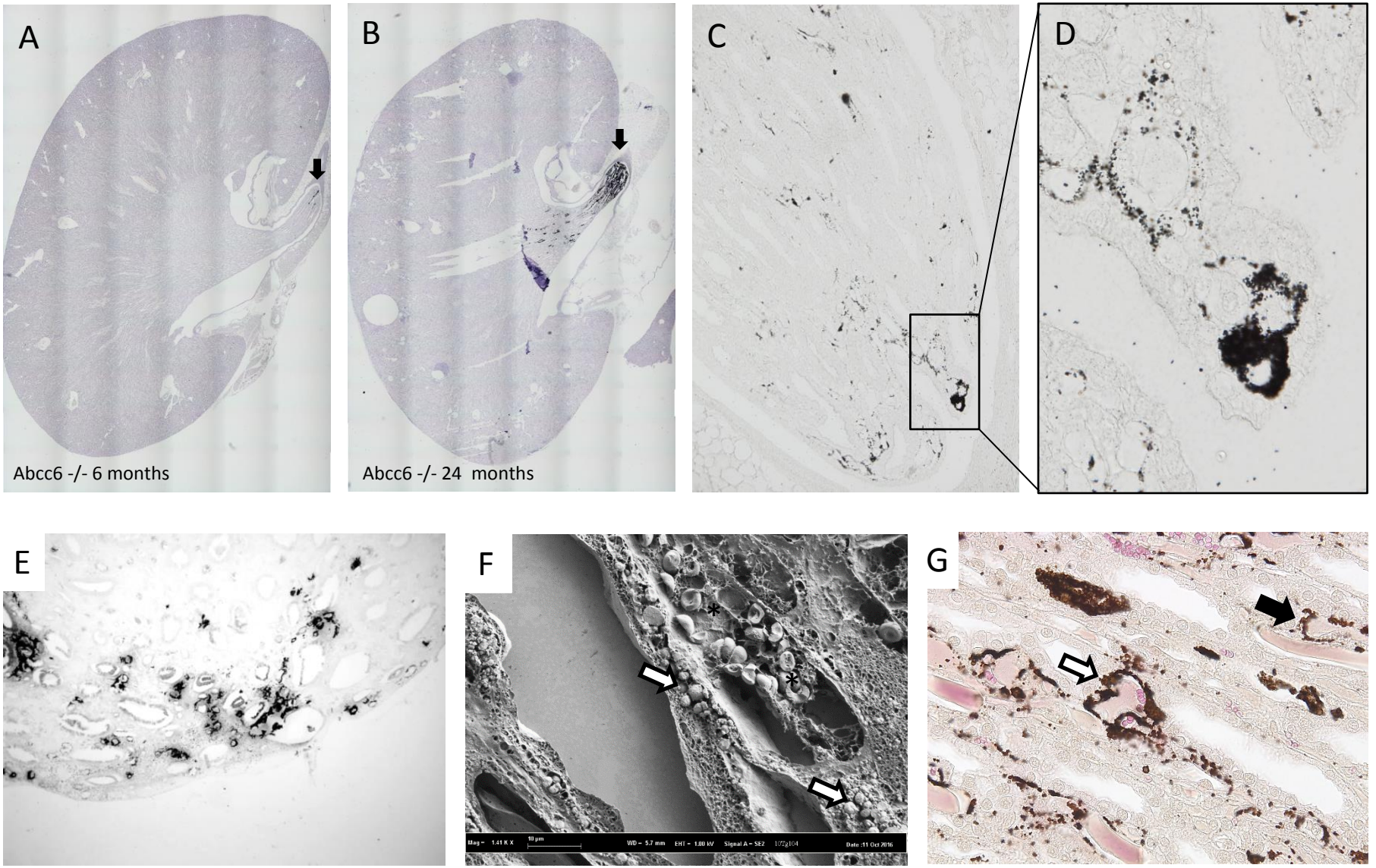
A
Abcc6 -/- 6 months
B
Abcc6 -/- 24 months
C
D
E
F
G

A

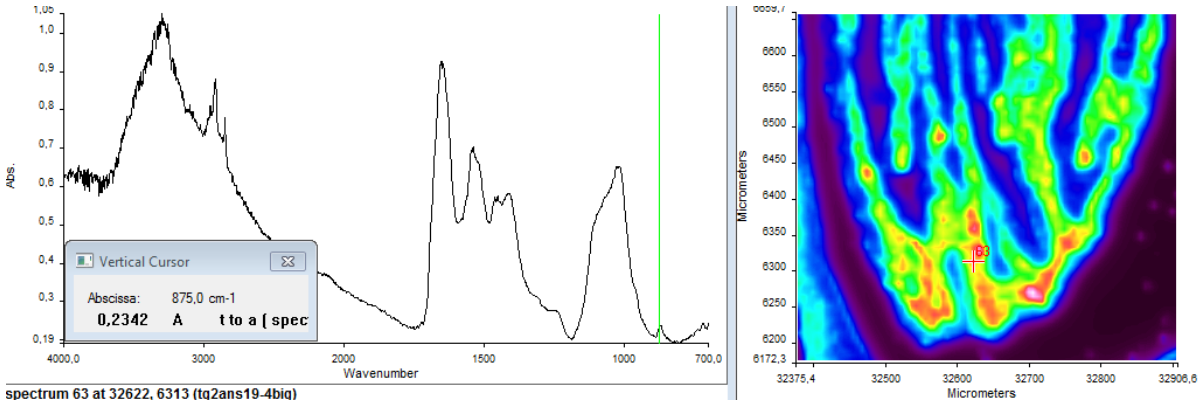
Vertical Cursor
Abscissa: 875,0 cm-1
0,2342 A t to a (spec
Abs.
Wavenumber
4000,0
3000
2000
1500
1000
700,0
Micrometers
32375,4
32500
32600
32700
32800
32906,6
spectrum 63 at 32622, 6313 (tq2ans19-4big)

B

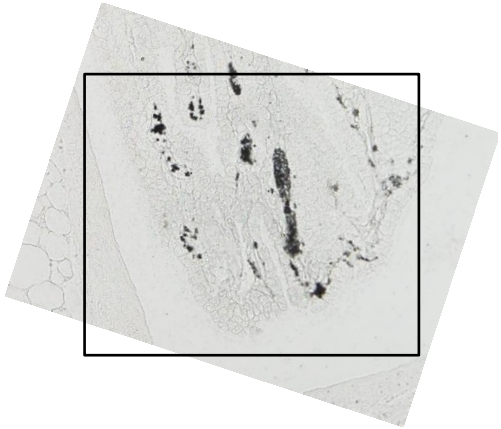

C

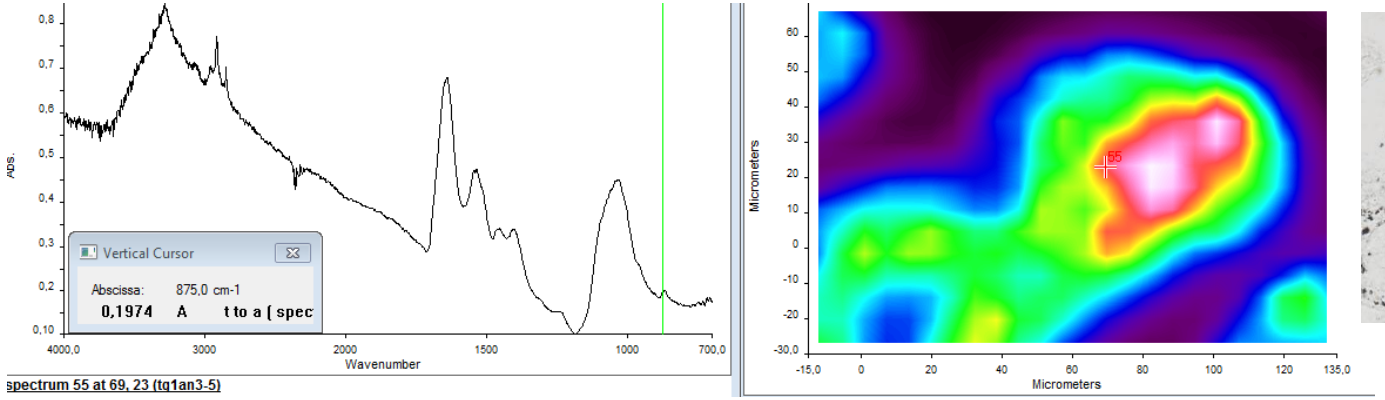
Vertical Cursor
Abscissa: 875,0 cm-1
0,1974 A t to a (spec
Abs.
Wavenumber
4000,0
3000
2000
1500
1000
700,0
Micrometers
-15,0
0
20
40
60
80
100
120
135,0
spectrum 55 at 69, 23 (tq1an3-5)

D

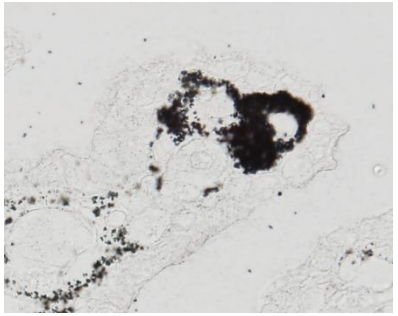

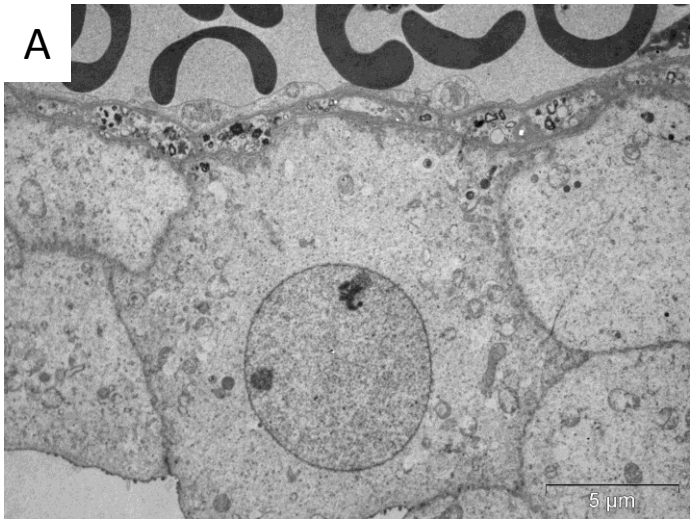
A
5 µm


B
500 nm

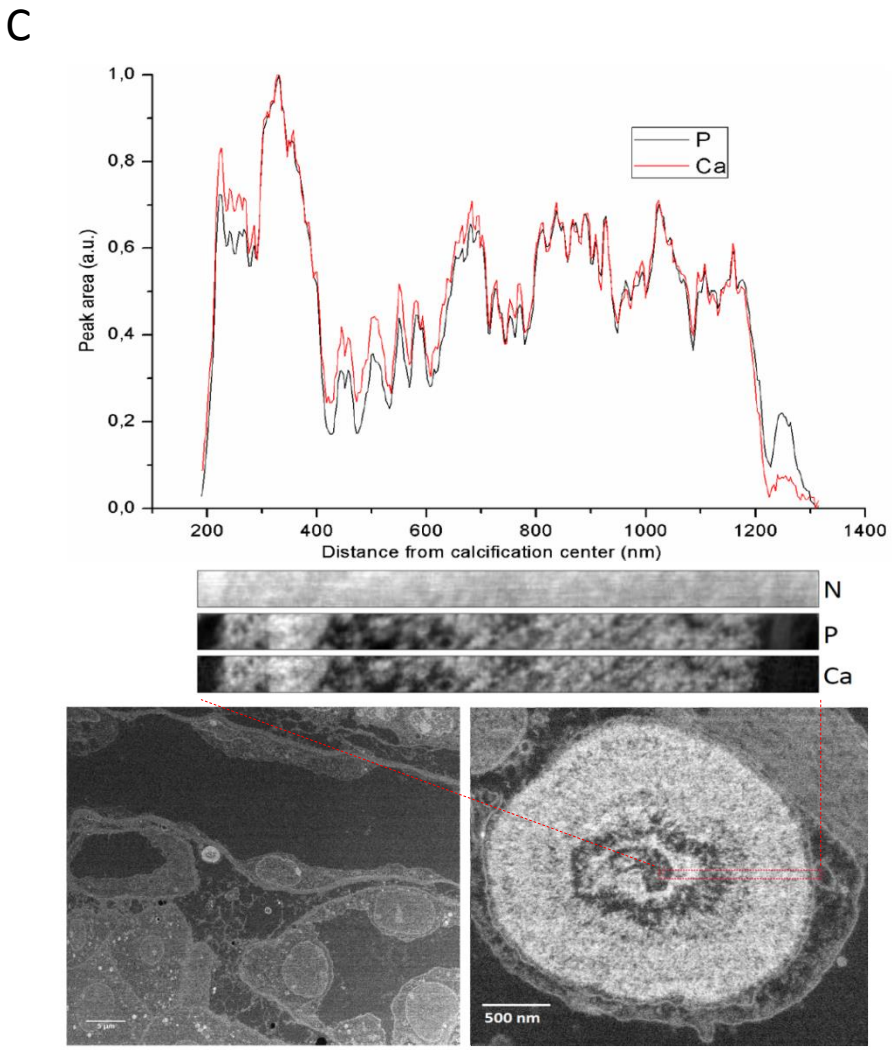
C
1,0
0,8
0,6
0,4
0,2
0,0
Peak area (a.u.)
200
400
600
800
1000
1200
1400
Distance from calcification center (nm)
P
Ca
N
P
Ca
500 nm

A

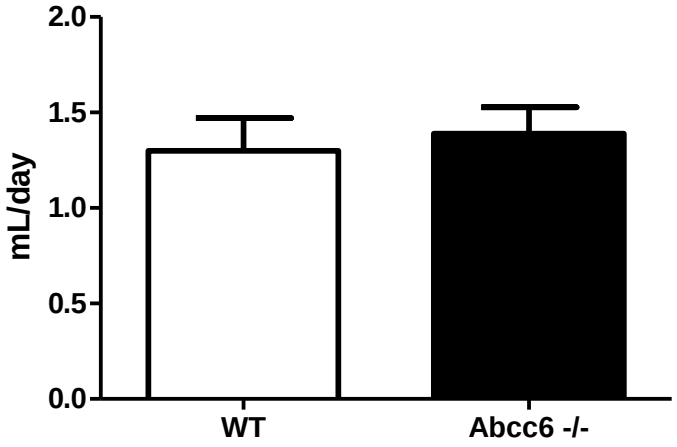
Urine volume/day
mL/day
2.0
1.5
1.0
0.5
0.0
WT
Abcc6 -/-

B

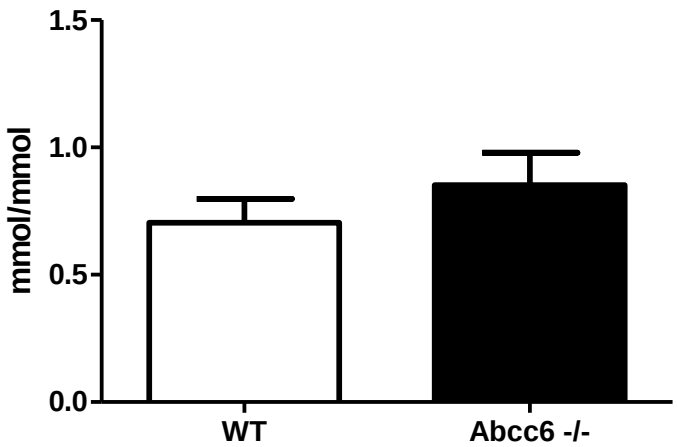
Urine calcium excretion
mmol/mmol
1.5
1.0
0.5
0.0
WT
Abcc6 -/-

C

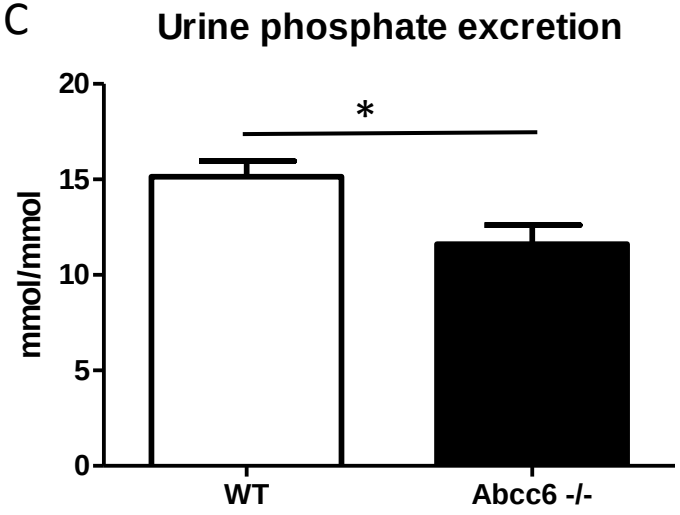
Urine phosphate excretion
mmol/mmol
20
15
10
5
0
*
WT
Abcc6 -/-

D

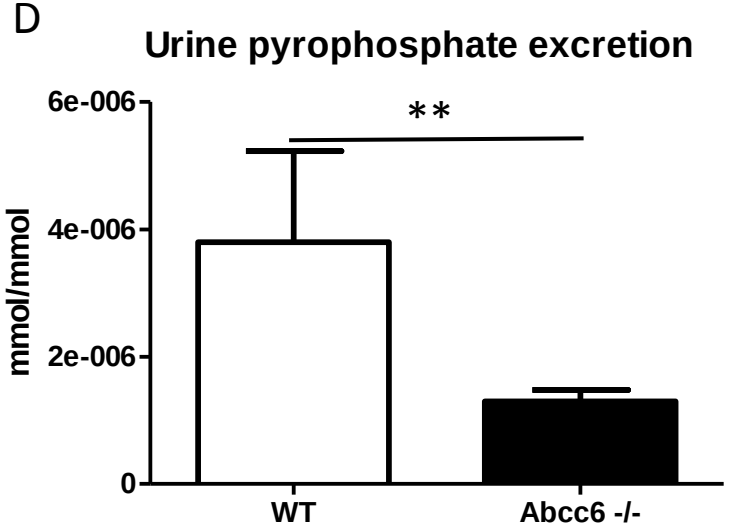
Urine pyrophosphate excretion
mmol/mmol
6e-006
4e-006
2e-006
0
**
WT
Abcc6 -/-

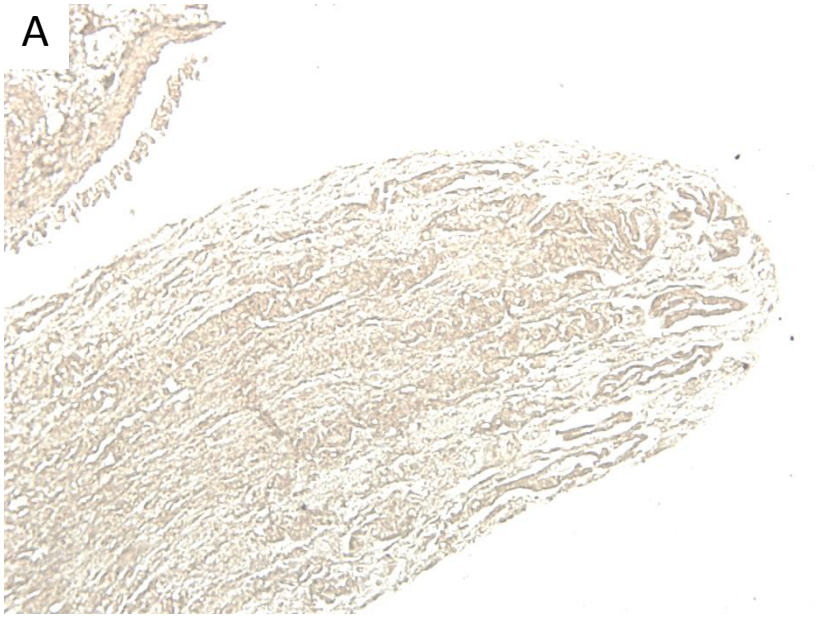
A

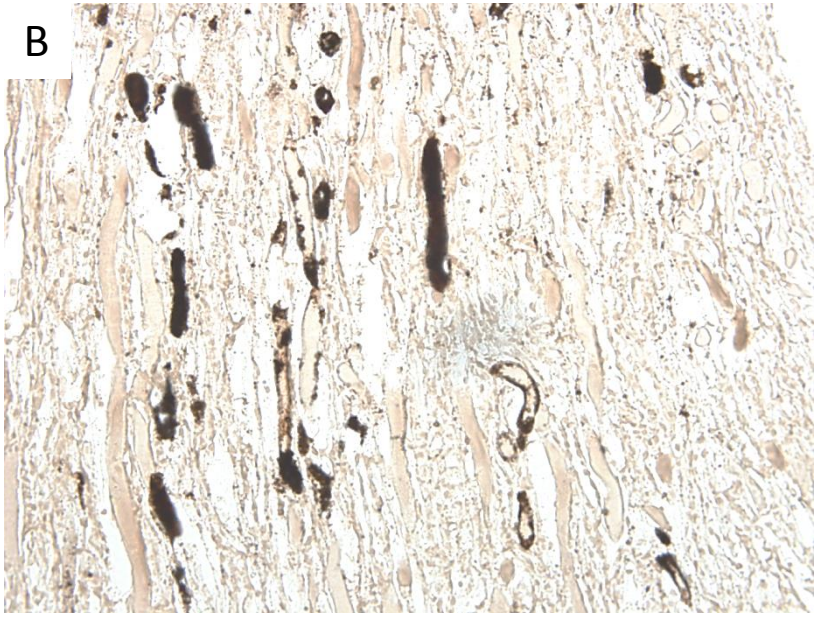
B

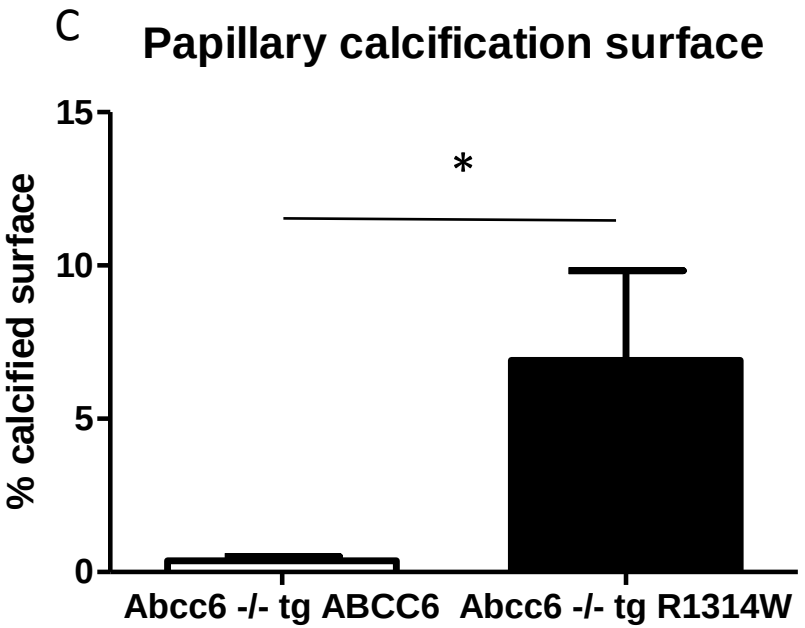
C
Papillary calcification surface
% calcified surface
15
10
5
0
*
Abcc6 -/- tg ABCC6
Abcc6 -/- tg R1314W